Laser and Particle Beams (2009), *27*, 137–147. Printed in the USA.

doi:10.1017/S0263034609000202

Experimental studies of generation of ~100 MeV Au-ions from the laser-produced plasma

L. LÁSKA,[1] J. KRÁSA,[1] A. VELYHAN,[1] K. JUNGWIRTH,[1] E. KROUSKÝ,[1] D. MARGARONE,[1,2] M. PFEIFER,[1] K. ROHLENA,[1] L. RYĆ,[3] J. SKÁLA,[1] L. TORRISI,[2,4] AND J. ULLSCHMIED[5]

[1]Institute of Physics, ASCR, v.v.i., Prague, Czech Republic
[2]Dipartimento di Fisica, Universita di Messina, Messina, Italy
[3]Institute of Plasma Physics and Laser Microfusion, Warsaw, Poland
[4]INFN-Laboratori Nazionali del Sud, Catania, Italy
[5]Institute of Plasma Physics, ASCR, v.v.i., Prague, Czech Republic

(RECEIVED 25 November 2008; ACCEPTED 2 December 2008)

Abstract

Using the PALS iodine laser system, Au ions with the charge state up to 58+ and with the kinetic energy as high as ~300 MeV were generated. The production of these ions was tested in dependence on the laser frequency (1ω, 3ω), on the irradiation/detection angles (0°, 30°), on the focus position with regard to the target surface, and on the target thickness (500 μm, 200 μm, 80 μm). A larger amount of the fastest ions was produced with 1ω than with 3ω, the most of the fast ions were recorded in the direction ~10° from the target normal, the optimum focus position is in front of the target and should be set on with a precision of 50 μm. The forward emission is weaker than the backward one for both of the thinner targets (which burn through) at our experimental conditions.

Keywords: Backward and forward ion emission; High energy Au-ions; Highly charged Au-ions; Laser-produced plasma

INTRODUCTION

Experiments performed up to now proved that the nonlinear processes, accompanying intense-laser interactions with preformed plasma, are significant additional (or even leading) mechanisms at a production of ions with very high characteristics (Láska *et al.*, 2005). The plasma, created by a slowly increasing front edge of a long (>100 ps) laser pulse, with which the main part of the pulse continues to interact, can be regarded as a kind of such preformed plasma. The characteristics of the produced ions differ, more or less, in dependence on various factors (Láska *et al.*, 2007). Among them, very important is the laser-beam focus position (FP) with respect to the target surface, which determines not only the nominal laser intensity, but also the length (duration) of the laser beam interaction with such a self-created plasma. Another important factor is the laser beam incidence angle onto the target (Láska *et al.*, 2008*a*). Third, target thickness determines the balance (possibility) between the backward direction of ion emission (from the front side of the target, against the laser beam) and the forward direction of ion emission (from the rear side, following the laser beam) (Badziak, 2007). With the intensity of laser radiation higher than $\sim 1 \times 10^{14}$ W/cm^2, the charge states and the energy of the generated ions, as well as their amount, increase due to the participation of ponderomotive, relativistic, or magnetic self-focusing (channeling, filamentation) of the laser beam, or due to other nonlinear effects occurring at such intensities (Hora, 1969, 1975; Hora *et al.*, 1978; Hauser *et al.*, 1992; Pukhov & Meyer-ter-Vehn, 1996; Borghesi *et al.*, 1997, 1998; Láska *et al.*, 2006). Experiments on the hydrodynamics of intense laser-produced plasmas, performed at the PALS laboratory, have been presented recently (Batani *et al.*, 2007).

This contribution is directed to the experimental investigation of the generation of ions with extreme characteristics, obtainable with the 1 kJ/300 ps iodine laser system PALS. Main attention was devoted to a determination of the highest attainable kinetic energy of ions and of the conditions at which they are produced. Simultaneously, the emission of hard X-rays was recorded and correlated with the generation of fast ions. An additional goal was to compare the ion emission and ion characteristics, when changing the target thickness. The reported results serve to identify and to discuss the mechanisms, participating in the generation (acceleration) of

Address correspondence and reprint requests to: L. Láska, Institute of Physics, ASCR, v.v.i., Na Slovance 2, 182 21 Prague 8, Czech Republic. E-mail: laska@fzu.cz

highly charged ions with extremely high kinetic energy, which have not yet been unambiguously identified. The conclusions should be useful for an optimization of the laser ion sources for pre-injectors of large heavy-ion accelerators, as well as for other scientific and/or technological purposes. Demands for collimated high currents of high-energy (fast) protons for inertial fusion experiments, and/or for (light) ions for medical use, make such investigations at present a real topic.

EXPERIMENTAL ARRANGEMENT

Our studies were performed using the PALS iodine high-power laser system in Prague (Jungwirth, 2005; Jungwirth *et al.*, 2001) with the fundamental ($\lambda = 1.315$ μm) and the 3rd harmonic ($\lambda = 0.438$ μm) frequencies, with laser energies up to ~400 J in a pulse < 300 ps long (full width in half maximum (FWHM)), and at variable focus positions (FP) with regard to the target surface. The convention used is that FP = 0 when the minimum focal spot coincides with the target surface, while FP < 0 means that it is located in front of the target surface, and FP >0 means that it is behind the target. The laser beam was focused onto the target with an aspherical lens of focal length $f =$ 627 mm for 1ω and $f = 600$ mm for 3ω. The minimum diameter of the focal spot of ~80 μm results in the attainable laser intensity of up to 5×10^{16} W/cm^2. While the intensity contrasts for the fundamental harmonics, 1ω is about 10^6 at ~1 ns prior to the laser pulse maximum, the energy ratio is only 10^2 at −0.5 ns. It means that, when taking into account, the integrated beam precursor during several hundreds of ps before the main part of the pulse, about 5 J of laser energy is deposited on the target to produce a pre-plasma (Ullschmied, 2006; Láska *et al.*, 2008*b*).

When irradiating the target perpendicularly, ions were detected at an angle of 30° with respect to the target normal, due to the target chamber construction (the angle between the input and output windows is 30°). The experimental chamber is sketched in Figure 1 (Torrisi *et al.*, 2008*a*). Changing the target tilt angle (laser beam incidence angle), the detection angle is automatically changed, too. Using thick (>1 mm) targets (slabs), the ions are emitted in the backward direction only (against the laser beam). When employing thinner targets and/or increasing significantly the laser intensity, the shape of produced craters changes (Torrisi *et al.*, 2003; Margarone *et al.*, 2008), the target starts to burn through and ions are emitted also (or mostly) forward (in the laser beam direction) (Maksimchuk *et al.*, 2000; Mackinnon *et al.*, 2001). To study this transition, altogether three thicknesses of the Au target (500 μm, 200 μm, 80 μm) were tested.

Two ion collectors of different constructions and a cylindrical electrostatic ion energy analyzer (IEA), based on the time-of-flight effect, were used for the ion diagnostics (Láska *et al.*, 1996; Woryna *et al.*, 1996). Measurements were performed in the far expansion zone (>1 m), where

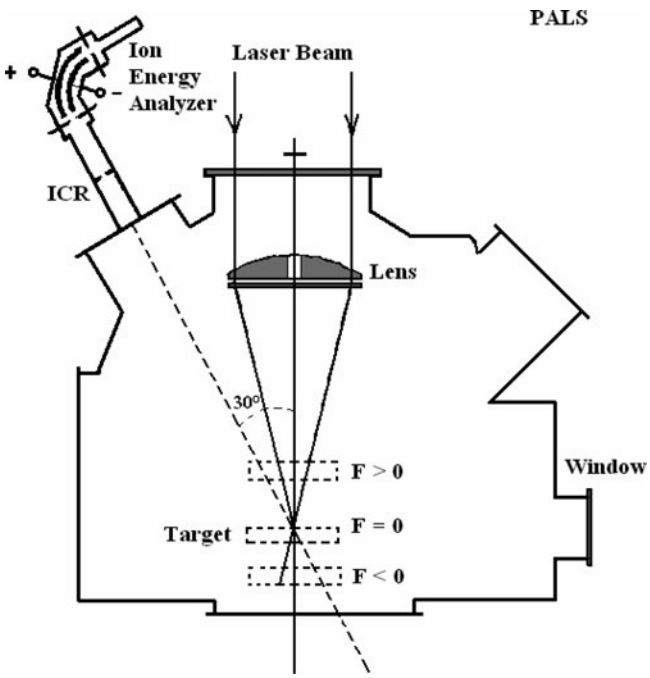

Fig. 1. View of the target chamber (scheme).

the ion charge-states are "frozen." The standard circular (flat) ion collector (IC3) with a variable entrance window (diameter 2.25 cm in this case) was the first one, the second one, a ring ion collector (ICR, $\varnothing_1 = 3.8$ cm, $\varnothing_2 =$ 5.0 cm), made possible the IC measurements close to the IEA axis. The grid transparency was 0.58. Both the collectors were negatively biased (~−100V). The IEA has a bending radius $R_0 = 10$ cm, the deflection angle $\Psi = 90^\circ$ and the gap between the cylindrical electrodes of the analyzing capacitor is $\Delta R = 0.5$ cm. Using the ± 10 kV voltage as a maximum on the electrodes of IEA, ions with energy-to-charge ratio up to $E_i/z =$ 200 keV can be detected. The path of flight L was 258 cm for IEA, 180 cm for ICR, and 165 cm for IC3, if the backward emitted ions were measured; it was 136 cm for ICR and for the forward emitted ions. For a better comparison, some of the ion collector signals were recalculated using relations $j = U/RST(1 + \gamma)$ and $j_1/j_2 = L_2^3/L_1^3$ to the current densities at the distance of 100 cm. U is the output IC voltage, the load resistance is $R = 25\Omega$, S is the IC surface, T is the IC grid transmission, γ is the coefficient of secondary electron emission induced by the impact of ions on the IC electrode, and z is the charge-state of the ions.

The IC measures the time-resolved, but charge-integrated signal, which can be expressed as $U(t) = R\ i(t) = R\ dQ/dt = R\ d(N(t)v < z(t) > e)/dt$, where $N(t) = \Sigma N_z(t)$ is the total number of ions involving all charge-states z at the instant t, $< z(t) > = < N_z(t)z(t) > / < N_z(t) >$ is the averaged charge-state of ions, e is the elementary charge. Since the measured ion current is a sum of partial currents due to various ionized species (which, moreover, may be produced by different mechanisms), both the magnitudes N and $<z>$

https://doi.org/10.1017/S0263034609000202 Published online by Cambridge University Press

can be determined only with the use of some kind of additional ion diagnostics (IEA, Thomson parabola spectrograph TPS (Woryna *et al.*, 1996)), or by completing it with a numerical deconvolution of the IC signal, containing a higher or lower number of peaks or humps, into a certain number of peaks (Krása *et al.*, 2007).

The IEA gives the possibility to identify the ion species produced; it determines the relative amount of single ions, having the same value of energy-to-charge state ratio E/z (at a fixed IEA voltage), their energy and abundance. The energy of ion species E_i (passing through the IEA) can be determined by using the relation $E_i = 2ze\kappa U/2$, where e is the elementary charge, κ is a device constant (10 in our case) and $\pm U/2$ are the declination voltages on IEA electrodes. Since our measurements were performed mostly with $U/2 = 1500$ V, a corresponding ion energy of $\sim$1.75 MeV was measured for the charge state of 58 +. The maximum detectable E_i depends on the maximum IEA voltage admitted.

Semiconductor photodiodes (Ryc *et al.*, 2003), thermoluminescent detectors TLD (Krása *et al.*, 2002), and CVD diamond detectors (Torrisi *et al.*, 2008*b*), all screened with various filters, monitored the X-ray radiation produced. For the detection of hard X-rays, a "FLM" type photodiode from ITE, Warsaw, was employed, the active-layer thickness of which was 380 μm, and a 307 μm Al foil as a filter. The hard radiation detector was sensitive in the range of 9.9 – 28 keV. For detection of the soft X-ray radiation, a "BPY03" type photodiode, also from ITE, Warsaw, was employed (the thickness of its active layer was about 2 μm) with the 5 μm Al-foil filter. This detector has two ranges of sensitivity: 0.8–1.6 keV and 2.1–6.3 keV. TLDs were screened with various X-ray filters to detect both the soft and hard X-rays.

RESULTS AND DISCUSSION

Experiments were performed first with a target thickness of 500 μm. Figure 2 shows an example of the IEA spectrum of Au ions, recorded at the third laser harmonic frequency 3ω, at the laser pulse energy $E_L \sim 170$ J, at the focus position FP = −200 μm, and for ions with the energy-to-charge ratio $E_i/z = 30$ keV. The highest $z_{max} = 58$ was found in the FP region from FP = −300 μm to FP = 0. Figure 3 demonstrates very illustratively the combined dependence of the detected charge states of ions on the angle of target irradiation (incidence) and on the angle of detection, recorded at 3ω, at $E_L = 170$ J, at FP = −100 μm, and for ions of $E_i/z = 30$ keV again. Generally, it is accepted that the main amount of the produced (fast) ions is emitted normally to the target (Ehler, 1975), up to 30° independently of the target incidence angle (Tallents *et al.*, 1986), with a narrow angular distribution, depending on the mass of the target (Buttini *et al.*, 1998), appearing even as a plasma jet long after the extinguishing of the heating laser pulse at some experimental conditions (Kasperczuk *et al.*, 2006, 2007, 2008). Other observed directions of the emitted ion groups can be explained only by admitting the presence of nonlinear processes in preformed plasma (Láska *et al.*, 2008*a*). Several ion groups are clearly seen in Figure 3, differing from each other in their charge state (they contain charges up to $\sim$15 +, up to $\sim$30 +, and up to 58+), and in the detection (incidence) angle. The record amount of ions with the highest charge state was recorded neither at the incidence angle $\Phi = 0°$ (irradiation perpendicularly to the target, the nominal laser intensity is maximal, but the angular distribution is narrower than the detection angle), nor at the incidence angle $\Phi = 30°$ (detection normally to the target, the laser intensity is lower according to cos Φ), but at $\Phi = \sim 20°$ ($\Theta \sim 10°$). Only a smaller secondary maximum was recorded at $\Theta = 0°$. This fact likely implicates the presence of nonlinear processes, namely the acceleration (and declination) of ions due to the indirect action of ponderomotive forces (which affect primarily the electrons).

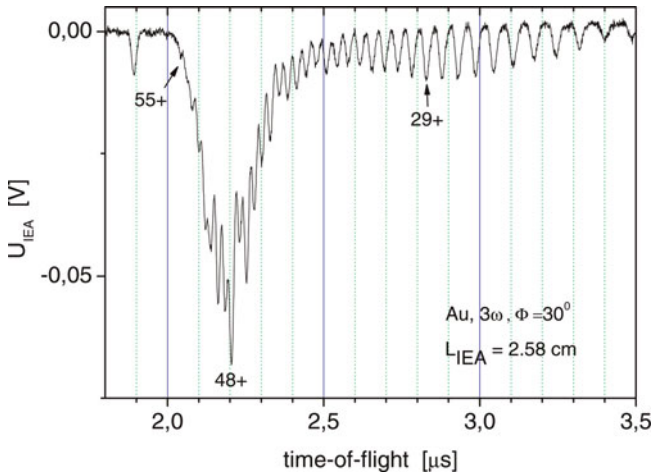

Fig. 2. IEA spectrum of Au ions obtained at 3ω, target thickness Δ = 500 μm, target tilt angle Φ = 30°, laser energy E_L = 172 J, focus position FP = −200 μm, $E_i/z = 30$ keV.

Generation of highly charged ions is strongly influenced by the focus position (by the corresponding value of the focus spot area). Generally, ions with the lower charge state (up to about 15 +) and lower kinetic energy are produced at lower laser intensities, and their production maxima are located more or less symmetrically on both sides from the exact focus FP = 0. This fact is attributed, similarly as the measured maxima of the soft X-rays, to larger focal spots and, therefore, to larger volumes of the plasma produced (Tallents *et al.*, 1986). With higher (increasing) laser intensities, a single pronounced maximum close to FP = 0 is typical for charge states from about 15 +. For charge states above 30 +, one or even more maxima appear, the FP distance between them is about hundred μm. The highest current peak is usually that observed close to FP = 0, but it is not a rule. At optimum focus position (FP < 0), more ions with the highest charge states and energy are produced than at FP > 0. It is ascribed

https://doi.org/10.1017/S0263034609000202 Published online by Cambridge University Press

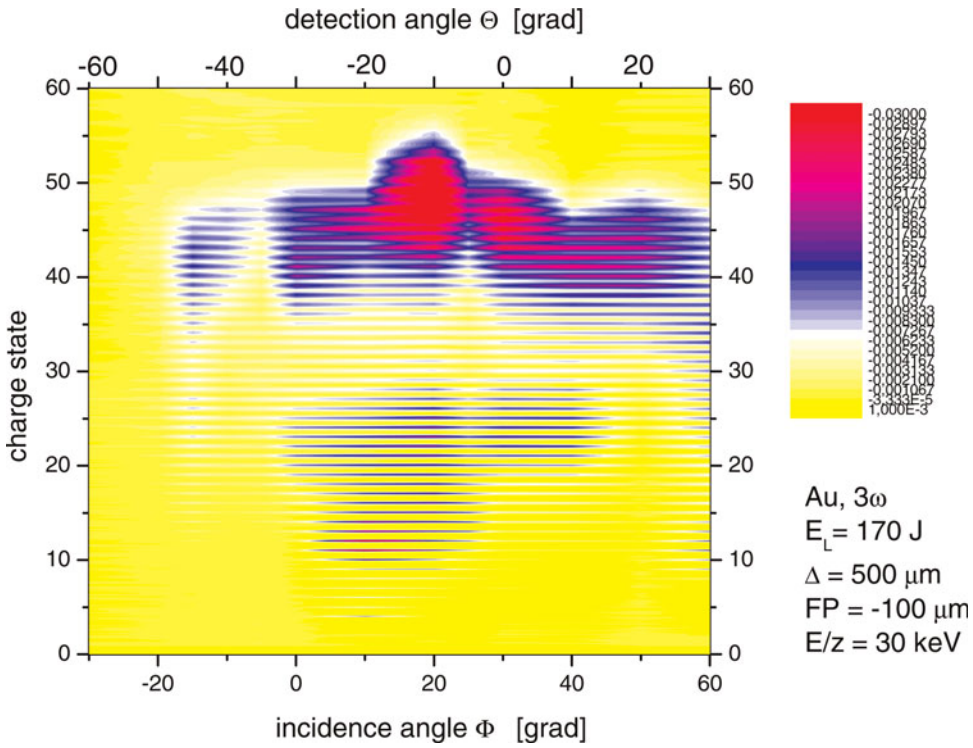

Fig. 3. (Color online) Au ion charge states recorded in dependence on the target tilt angle Φ (3ω, $\Delta = 500$ μm, $E_L = 170$ J, FP $= -200$ μm, $E_i/z = 30$ keV).

to a more favorable focus location with regard to the expanding plasma plume and, consequently, to a more effective self-focusing process.

An example of values of the generated ion charge states in dependence on the focus position from FP $= -600$ μm to FP $= +500$ μm (at 1ω, $E_L = 370$ J, $E_i/z = 30$ keV), is presented in Figure 4. A small current of ions with $z_{max} \sim 55+$ was recorded at FP $= +200$ μm in that case. The absolutely largest amount of highly charged ions with the charge states from $\sim 40+$ to $50+$ (peak signal at FP $= -450$ μm), in addition to several smaller maxima, are again supposed to be due to the presence of nonlinear processes. The distances between those maxima copy (qualitatively, at least) similar distances of hard X-rays maxima, measured simultaneously (Láska *et al.*, 2008*c*). For a thorough quantitative comparison, it would be necessary to measure the charge-energy distribution for each FP. The kinetic energy of ions with the charge state $50+$ is 1.5 MeV only, which is not the highest one observed.

Another possibility to determine E_i by using the IEA (considering limitations mentioned in Experimental Arrangement) means to estimate (calculate) it from the IC signal. The IC signal consists of a response to the X-ray radiation, hitting the IC first (a narrow, at some conditions line-like photo-peak, which determines the beginning of the IC signal), and of a more or less narrow, exponentially decreasing signal, with or without some (small) peaks superimposed on it, as it is seen in Figure 5 at IC signal recorded for 1ω at $\Phi = 0^\circ$ (10 V ~ 100 mA/cm^2 at $L = 1$ m). However, the shape of the curve may look quite differently at different experimental conditions; such signals pass through a minimum (usually at short times, < 1 μs in the far expansion zone > 1 m), followed by smaller or larger humps and maxima, depending on the relevant ion production and acceleration mechanisms (as it is seen in Fig. 5 for IC signal at 3ω and $\Phi = 30^\circ$). A careful analysis of the initial part of the IC signals (variable course of that decreasing part in dependence on the laser intensity and on the focus position, significant maxima distinguishable even at the time delay around 0.1 μs from the photo-peak) suggests that this part corresponds to the ions with the highest velocity. According to the relation E_i [keV] $= 5.18 A\, v^2$ (10^8 cm/s) (A is the atom mass), the time-of-flight peak at 0.2 μs means the ion velocity 9×10^8 cm/s, and the energy per mass unit $E_i/u =$ 419 keV/u. This value corresponds, in fact, to the energy of fast protons (hydrogen present from impurities), but also to the energy $E_i = 82.6$ MeV of the Au ions. The IC signals, acceptable even at time positions shorter than 0.1 μs, indicate the velocities above 1.8×10^9 cm/s, which represent a kinetic energy of Au ions above $E_i \sim 330$ MeV. It is in agreement with the similar results in Haseroth and Hora (1996) ($A = 181$ is presented there as Au). Haseroth and Hora (1996) and Hora *et al.* (1978) have predicted such huge values of heavy ion energies, due to relativistic self-focusing. Experimentally they were observed and reported by Clark *et al.* (2000). Figure 6 demonstrates the changes of the shape of IC signals in dependence on the focus positions at 3ω, $\Phi = 30^\circ$, and $E_L = 170$ J. The largest amount of fast ($v > 1 \times 10^8$cm/s) and the most

https://doi.org/10.1017/S0263034609000202 Published online by Cambridge University Press

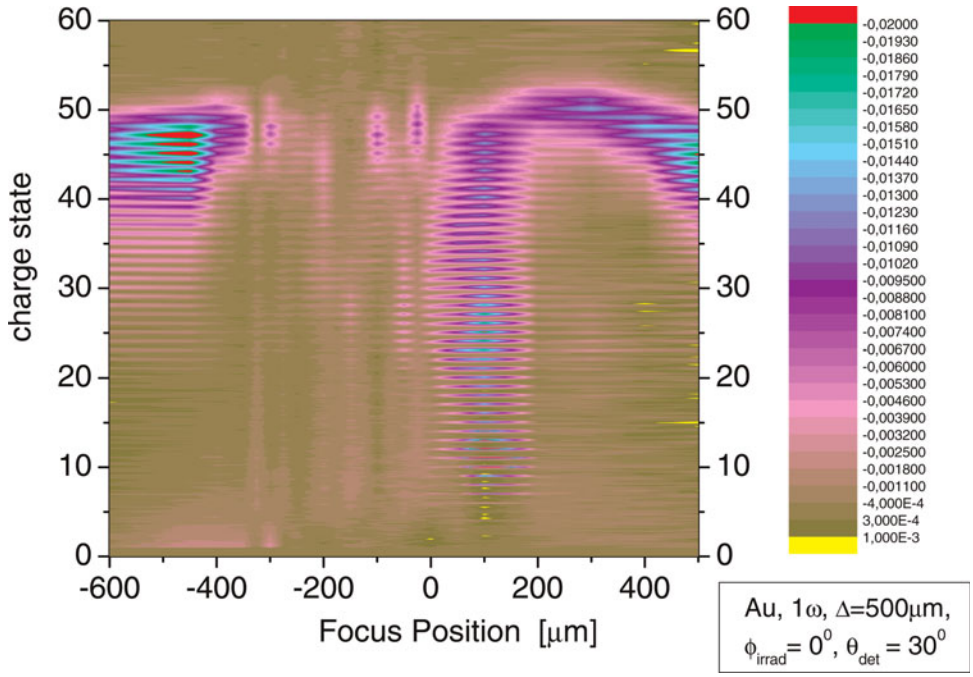

Fig. 4. (Color online) Au ion charge states recorded in dependence on the focus position FP (1ω, $\Delta = 500$ μm, $\Phi = 0^{\circ}$, $E_L = 170$ J, $E_i/z = 30$ keV).

energetic Au ions were produced at FP $= -150$ μm (i.e., in front of the target), while the lowest emission was found at FP $= 0$. Worth noticing are the surprisingly large changes, observed for short FP steps of 50 μm only.

The influence of the target thickness Δ on the ion production was examined by using 200 μm and 80 μm thick Au foils, which burn through at our experimental conditions. Ion collectors were located on both the front and the rear

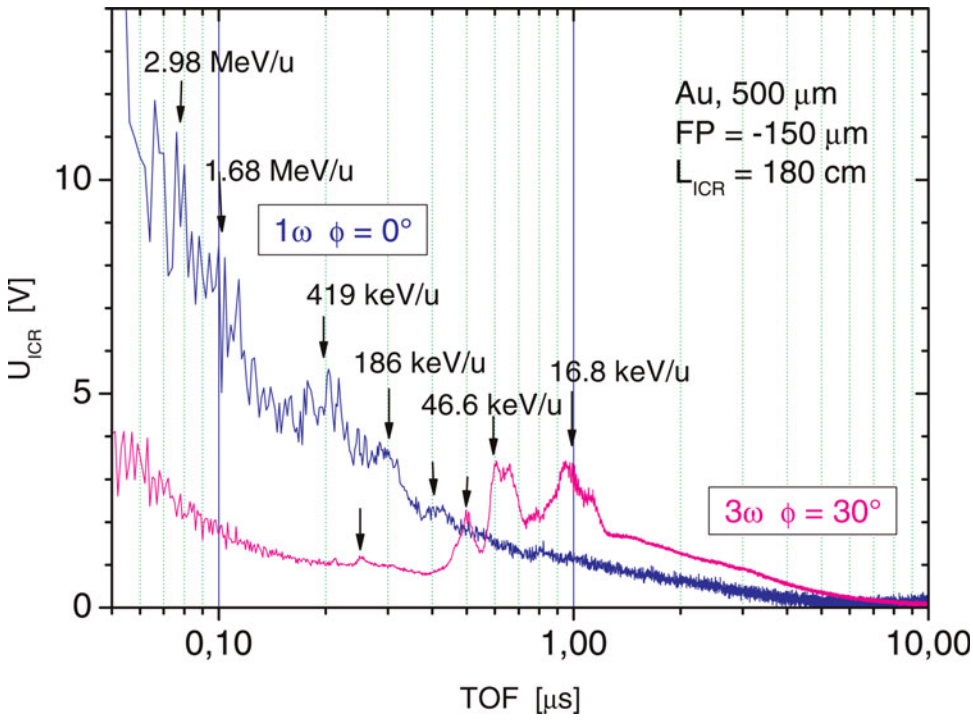

Fig. 5. (Color online) Ion collector signals recorded at 1ω, $\Phi = 0^{\circ}$, $E_L = 370$ J and at 3ω, $\Phi = 30^{\circ}$, $E_L = 170$ J (Au, $\Delta = 500$ μm, FP $= -150$ μm).

https://doi.org/10.1017/S0263034609000202 Published online by Cambridge University Press

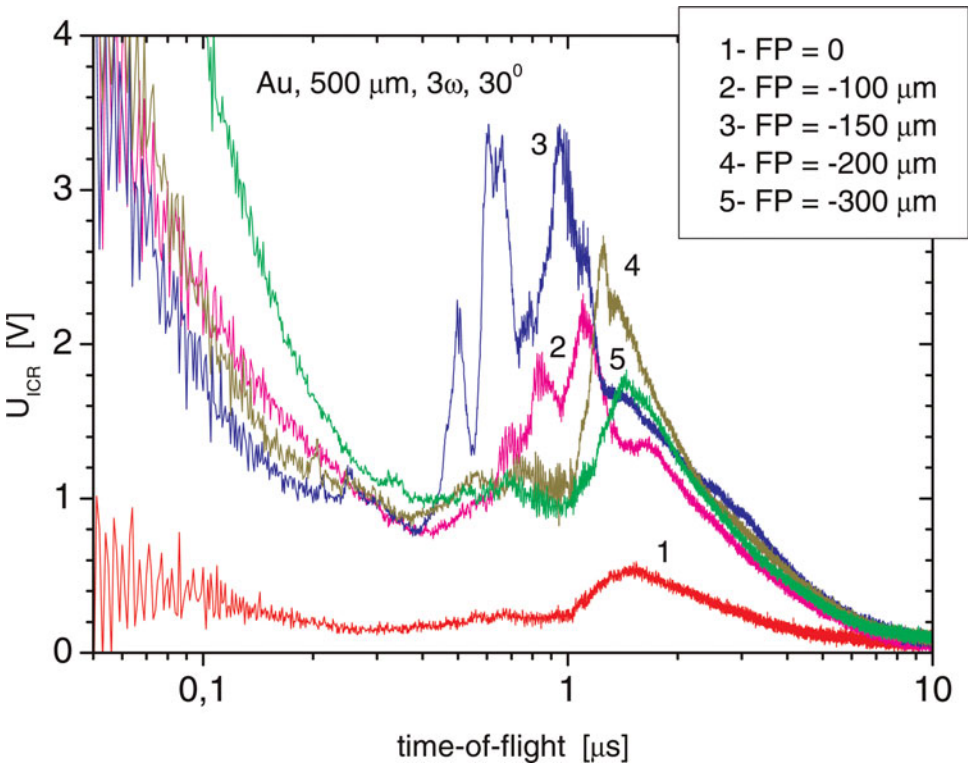

Fig. 6. (Color online) Ion collector signals recorded in dependence on the focus position FP (Au, $\Delta = 500$ μm, 3ω, $\Phi = 30^{\circ}$, $E_L = 170$ J).

sides of the target, in the target normal direction. The amplitudes of IC signals were recalculated to the current densities j at a distance of 1 m. The recalculated currents for the target of 200 μm thickness, obtained at 1ω, at $\Phi = 30^{\circ}$, at $E_L = 390$ J, and at two focus positions (FP $= -100$ μm and -200 μm), are presented in Figure 7. The total amount of ions produced from the rear side (forward emission) is much smaller than that from the front side (backward emission), in particular

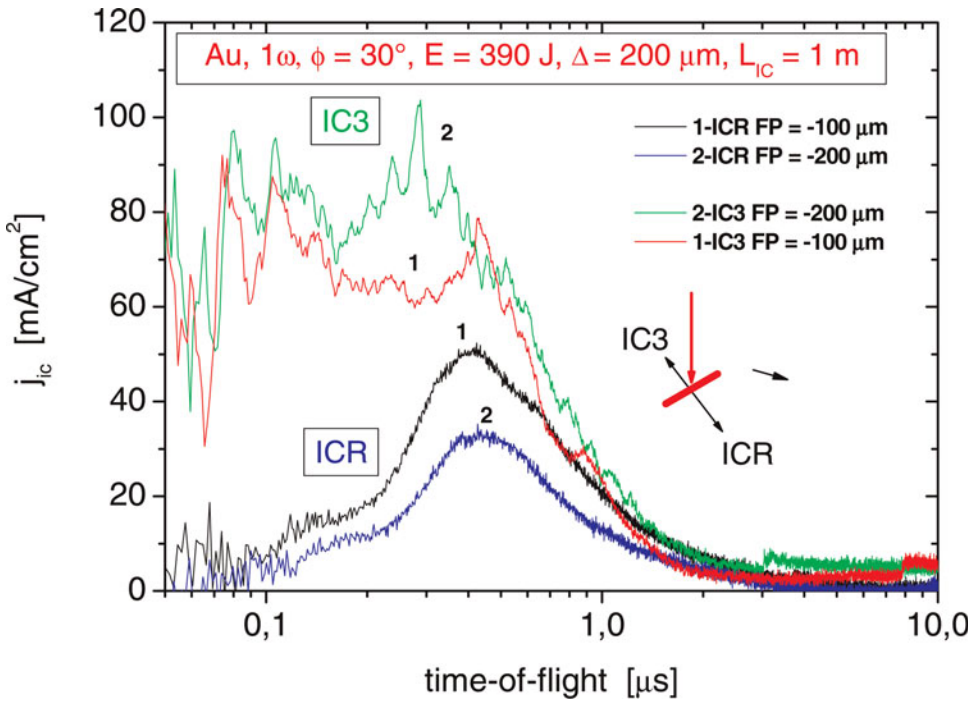

Fig. 7. (Color online) Ion collector signals of backward and forward emissions in dependence on the focus position FP (Au, $\Delta = 200$ μm, 1ω, $\Phi = 30^{\circ}$, $E_L = 390$ J).

https://doi.org/10.1017/S0263034609000202 Published online by Cambridge University Press

for the fastest ions. The peak ion current density of the fast forward Au ions, generated at FP = +50 μm (in Fig. 8), is $j_{max} \sim 30$ mA/cm^2, while the backward ion emission is about three times higher for the same focus position. The energy per mass unit of ions at this peak is 29.4 keV/u. In the part corresponding to the ions with the energy around 1 MeV/u, this ratio increases to 10. It means that the main differences in backward and forward ion emission at these experimental conditions are significantly larger amount and energy of backward emitted fast ions. This relation between both the currents persist, in principle, even if the focusing is varied from the focus position FP = +200 μm to FP = −500 μm. The forward emission is maximal at FP = −100 μm (see Fig. 9), proving that the burn-through is the fastest in this case, but the forward emission is not as effective as the backward one.

The situation for 80 μm foil looks a little bit different. The signals shown in Figure 10, with maximum current density of backward emission ~100 mA/cm^2, were recorded at 1ω, at $\Phi = 30^\circ$, at $E_L = 416$ J, and at FP = +50 μm. At these experimental conditions, the burn-through is much faster, and the emission from the rear side seems to be almost comparable with that from the front side, even for the focus located behind the target (FP > 0). As for the front (backward) emission, a strong dependence on the FP was found (see Fig. 11). With the FP increasing in the minus direction (FP < 0), the amount of the fast ions strongly decreases, and the fastest ions disappear (in contrast to the focus position dependence shown in Fig. 6). At FP < −300 μm, most of the Au ions are produced with the mean ion energy of about 10 keV only. This can be explained by the fact that the conditions for self-focusing are not fulfilled due to the fast burn-through of the target. Then a large hole is created and forward emission prevails.

Ions in laser-produced plasma can be accelerated by various mechanisms, all of which are associated primarily with the generation, properties, and behavior of the electrons. The thermokinetic (gas-dynamic) and electrostatic forces are usually responsible for generation of the low-energy ions (<100 keV). The high-energy ions are accelerated due to the electromagnetic (electrostatic-like and ponderomotive) forces (Badziak, 2007). The electrostatic forces are created because of separation of electrons and ions in the plasma due to the action of thermokinetic forces, or induced by various nonlinear processes. Since the electric field may attain values of TV/m (Malka *et al.*, 2008), it means that the charge-separated ions can be accelerated even to an energy ~100 MeV along the Debye-length distance (~ 1 μm). The ponderomotive forces are induced by inhomogeneity of the laser field in the plasma, usually because of inhomogeneous space distribution of plasma density. In the simplest case, the ponderomotive forces are proportional to the gradient of electromagnetic energy in the plasma (Badziak, 2007). Because of a great difference in the electron and ion masses, the ponderomotive force acts, in reality, directly on electrons only. Ions are then efficiently accelerated indirectly by the electric field created because of charge separation due to that force.

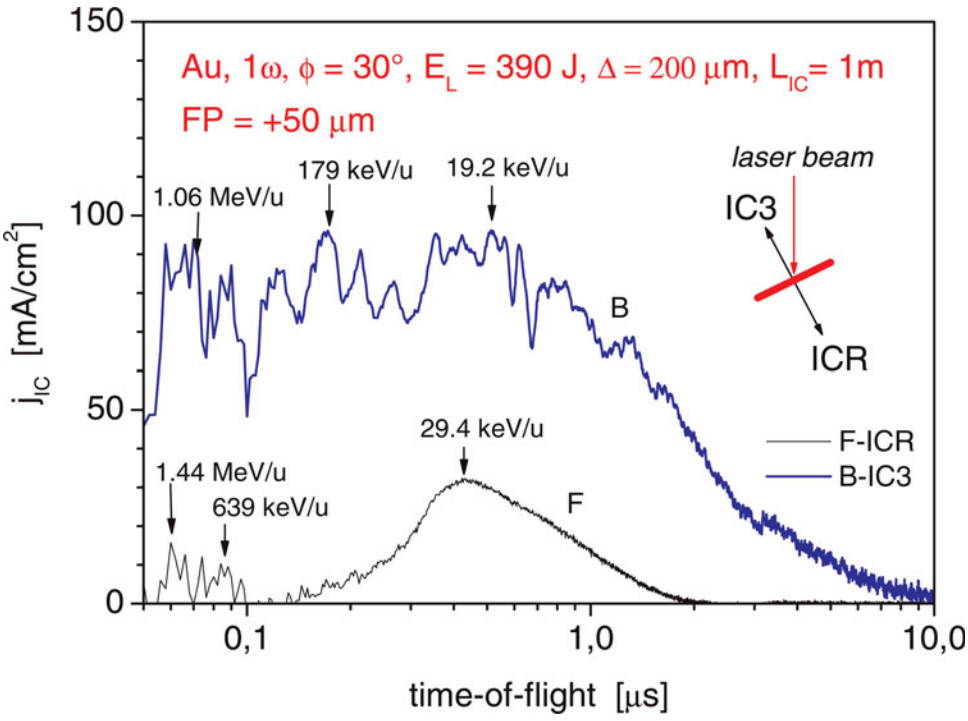

Fig. 8. (Color online) Comparison of ion collector signals of backward and forward emissions (Au, Δ = 200 μm, 1ω, $\Phi = 30^\circ$, E_L = 390 J, FP = +50 μm).

https://doi.org/10.1017/S0263034609000202 Published online by Cambridge University Press

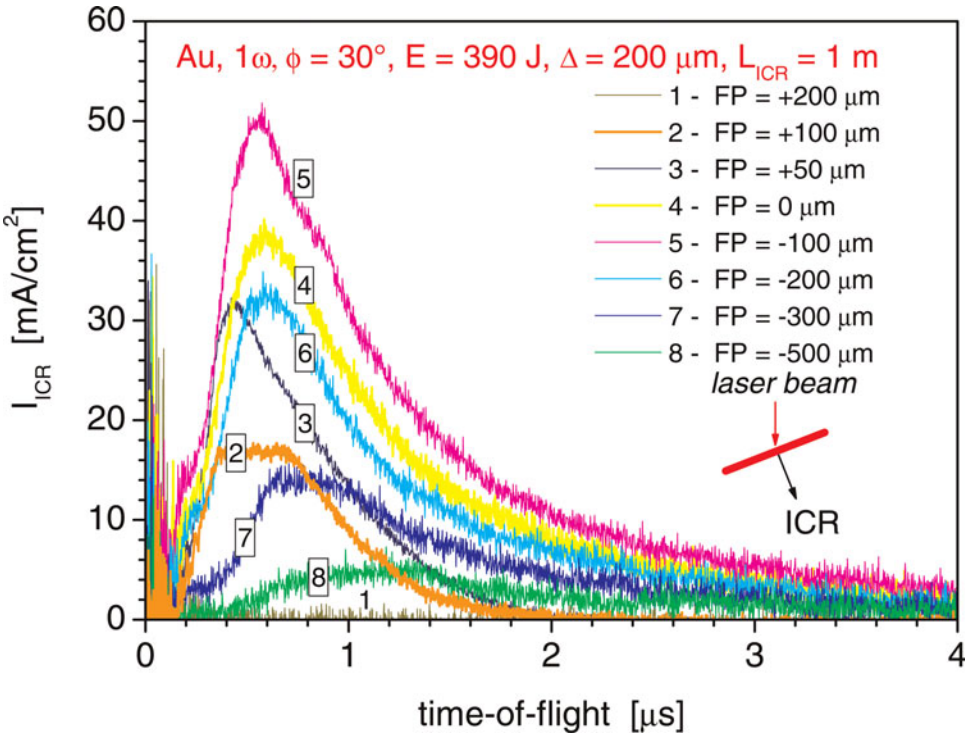

Fig. 9. (Color online) Ion collector signals of forward emission in dependence on the focus position FP (Au, $\Delta = 200$ μm, 1ω, $\Phi = 30^{\circ}$, $E_L = 390$ J).

The laser power threshold for ponderomotive self-focusing is ∼1 MW. If a Nd-laser beam of intensity exceeding the value $I = 3 \times 10^{15}$ W/cm^2 ($I\lambda^2 \sim$const. for other wavelengths) is incident on a target, the relativistic self-focusing occurs and the laser beam diameter shrinks down to about λ within the length L_{SF} comparable with the initial laser beam diameter (Hora *et al.*, 1978). A short-range shrinking of a laser beam generates intensities $I = P/\lambda^2$, which

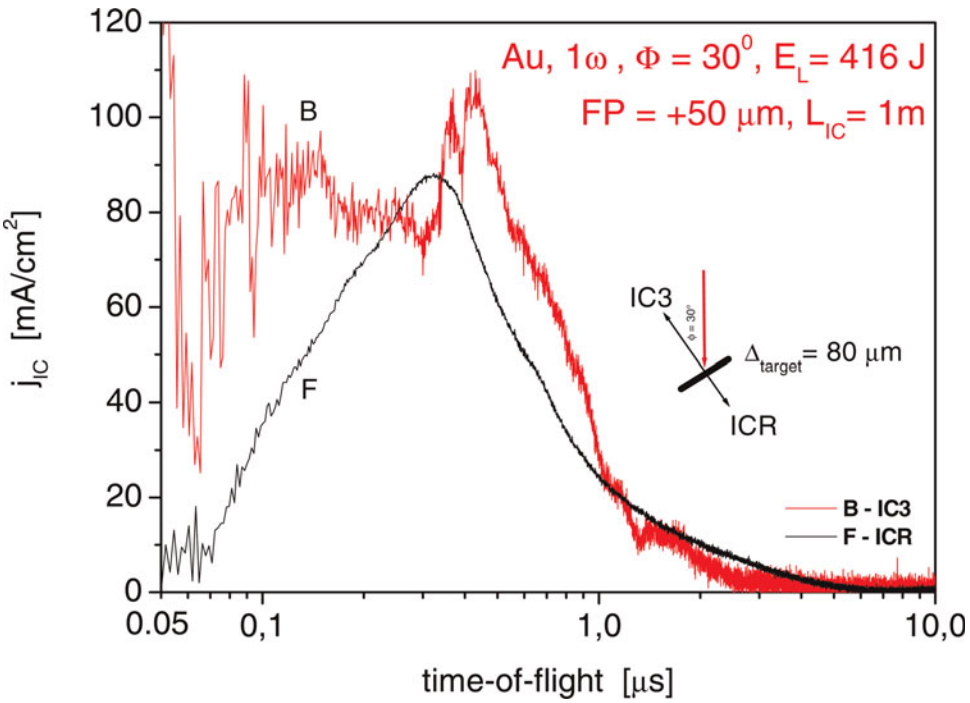

Fig. 10. (Color online) Comparison of ion collector signals of backward and forward emissions (Au, $\Delta = 80$ μm, 1ω, $\Phi = 30^{\circ}$, $E_L = 416$ J, FP = +50 μm).

https://doi.org/10.1017/S0263034609000202 Published online by Cambridge University Press

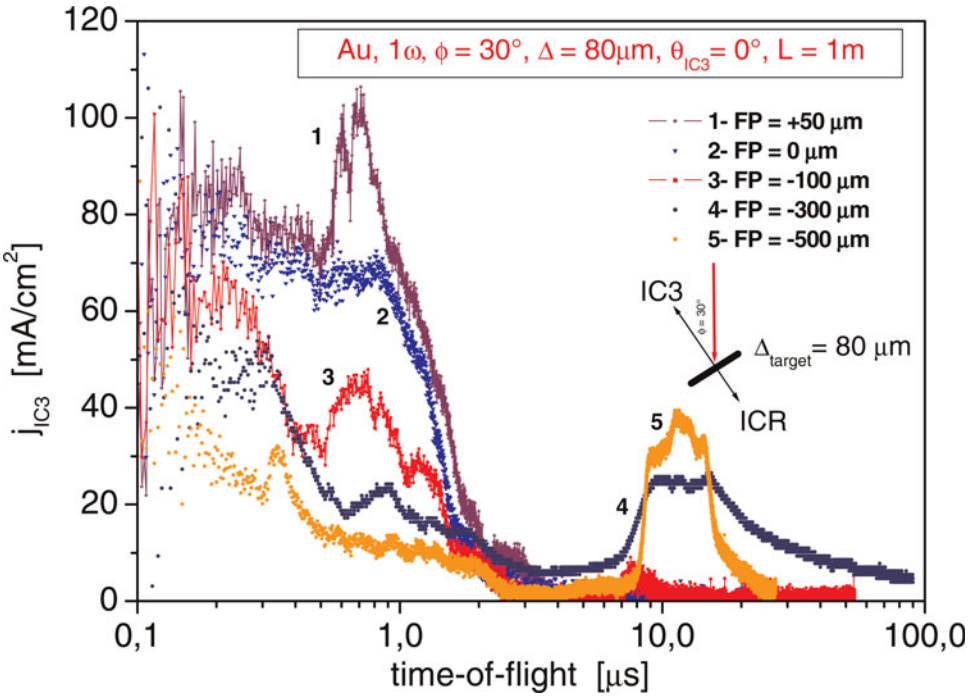

Fig. 11. (Color online) Ion collector signals of backward emission in dependence on the focus position FP (Au, $\Delta = 80$ μm, 1ω, $\Phi = 30^{\circ}$, $E_L = 390$ J).

accelerate highly charged ions above MeV energies. A decreasing laser beam diameter results in a significant increase in the radial components of both ponderomotive and thermokinetic forces in the plasma.

Huge electromagnetic fields induced in the plasma by the laser pulse can accelerate electrons to relativistic velocities. The oscillatory energy of electrons in the laser field (depending on the laser intensity) induces an acceleration of z-times ionized ions leading to the kinetic energy given by E_i (eV) $= 3.1 \times 10^{-6} \times ZxP(W)$, independent of the laser wavelength (the relation is valid for subrelativistic ion energies only, the validity limit is $v_{max} = c/2$) (Hora *et al.*, 1978). When using this relation and considering conditions of our experiment, the calculated ion energies of Au ions should be around 175 MeV, and of the fast protons∼3 MeV, in a full correspondence with the recorded ones.

CONCLUSIONS

Comparing different conditions of our experiment, the results can be summarized in the following way. Highly charged Au ions with charge states above 50+ and with the kinetic energy above 100 MeV, can be generated using both the 1ω and 3ω harmonics of iodine laser. Due to the precursor of the laser pulse at the fundamental frequency, better conditions for laser interactions with the self-created pre-plasma are established. The critical density is lower, more fast electrons are produced, and the threshold power density for the relativistic self-focusing is lower, too. For the third harmonic frequency, the precursor is removed, the plasma is denser, and collision dominated. Moreover, the power density threshold for the self-focusing goes up by an order of magnitude. However, focusing with the blue light is tighter. Since the generation of the fast electrons is less likely for the nominal laser intensity at 3ω, we also attribute their generation to the onset of self-focusing.

The laser pulse precursor and the illumination geometry (incidence angle, focus position, extraction angle) play a key role in the processes of generation and detection of ions with the extreme characteristics. Au ions with the kinetic energy in a region of ∼300 MeV and with the maximum charge-states 58+ were recorded. The current density may reach the values higher than ∼100 mA/cm^2 at a 1 m distance. The front side (backward) emission of the fastest ions is the strongest for a focus position of about 100 μm in front of the target, and for a target thickness of 200 μm.

ACKNOWLEDGMENT

This research was kindly supported by the Grant Agency of the ASCR, v.v.i. (grant No. IAA 100100715).

REFERENCES

Badziak, J. (2007). Laser-driven generation of fast particles. *Opt. Electr. Rev.* **15**,1–12.

Batani, D., Dezulian, R., Redaelli, R., Benocci, R., Stabile, H., Canova, F., Desai, T., Lucchini, G., Krousky, E., Masek, K., Pfeifer, M., Skala, J., Dudzak, R., Rus, B., Ullschmied, J., Malka, V., Faure, J., Koenig, M., Limpouch, J., Nazarov, W.,

https://doi.org/10.1017/S0263034609000202 Published online by Cambridge University Press

Pepler, D., Nagai, K., Norimatsu, T. & Nishimura, H. (2007). Recent experiments on the hydrodynamics of laser-produced plasmas conducted at the PALS laboratory. *Laser Part. Beams* **25**, 127–141.

Borghesi, M., MacKinnon, A.J., Barringer, L., Gaillard, R., Gizzi, L.A., Meyer, C., Willi, O., Pukhov, A. & Meyer-ter-Vehn, J. (1997). Relativistic channeling of a picosecond laser pulse in a near-critical preformed plasma. *Phys. Rev. Lett*. **78**, 879–882.

Borghesi, M., MacKinnon, A.J., Gaillard, R., Willi, O., Pukhov, A. & Meyer-ter-Vehn, J. (1998). Large quasistatic magnetic fields generated by a relativistically intense laser pulse propagating in a preformed plasma. *Phys. Rev. Lett*. **80**, 5137–5140.

Buttini, E., Thum-Jager, A. & Rohr, K. (1998). The mass dependence of the jet formation in laser-produced particle beams. *J. Phys. D* **31**, 2165–2169.

Clark, E.L., Krushelnik, K., Zepf, M., Beg, F.N., Tatarakis, M., Machacek, A., Santala, M.I.K., Watts, I., Noreys, P.A. & Dangor, A.E. (2000). Energetic heavy–ion and proton generation from ultraintense laser-plasma interactions with solids. *Phys. Rev. Lett*. **85**, 1654–1657.

Ehler, A.W. (1975). High-energy ions from a CO_2 laser-produced plasma. *J. Appl. Phys*. **46**, 2464–2467.

Haseroth, H. & Hora, H. (1996). Physical mechanisms leading to high currents of highly charged ions in laser-driven ion sources. *Laser Part. Beams* **14**, 393–438.

Hauser, T., Scheid, W. & Hora, H. (1992). Theory of ions emitted from a plasma by relativistic self-focusing of laser beams. *Phys. Rev*. **A45**, 1278–1281.

Hora, H. (1969). Self-focusing of laser beams in a plasma by ponderomotive forces. *Z. Physik* **226**, 156–159.

Hora, H. (1975). Theory of relativistic self-focusing of laser radiation in plasma. *J. Opt. Soc. Am*. **65**, 882–886.

Hora, H., Kane, E.L. & Hughes, J.L. (1978). Generation of MeV ions by relativistic self-focusing from laser-irradiated targets. *J. Appl. Phys*. **49**, 923–924.

Jungwirth, K. (2005). Recent highlights of the PALS research program. *Laser Part. Beams* **23**, 177–182.

Jungwirth, K., Cejnarová, A., Juha, L., Králiková, B., Krása, J., Krouský, E., Krupicková, P., Láska, L., Mašek, K., Mocek, T., Pfeifer, M., Präg, A., Renner, O., Rohlena, K., Rus, B., Skála, J., Straka, P. & Ullschmied, J. (2001). The Prague Asterix Laser System PALS. *Phys. Plasmas* **8**, 2495–2501.

Kasperczuk, A., Pisarczyk, T., Borodziuk, S., Ullschmied, J., Krouský, E., Mašek, K., Rohlena, K., Skála, J. & Hora, H. (2006). Stable dense plasma jets produced at laser power densities around 10^{14} W/cm^2. *Phys. Plasmas* **13**, 062704.

Kasperczuk, A., Pisarczyk, T., Borodziuk, S., Ullschmied, J., Krouský, E., Mašek, K., Pfeifer, M., Rohlena, K., Skála, J. & Pisarczyk, P. (2007). Interferometric investigations of influence of target irradiation on the parameters of laser-produced plasma jets. *Laser Part. Beams* **25**, 425–434.

Kasperczuk, A., Pisarczyk, T., Kalal, M., Martinkova, M., Ullschmied, J., Krousky, E., Masek, K., Pfeifer, M., Rohlena, K., Skala, J. & Pisarczyk, P. (2008). PALS laser energy transfer into solid targets and its dependence on the lens focal point position with respect to the target surface. *Laser Part. Beams* **26**, 189–196.

Krása, J., Cejnarová, A., Juha, L., Ryć, L., Scholz, M. & Kubeš, P. (2002). Semiconductor and thermoluminescent dosimetry of pulsed soft X-ray plasma sources. *Radiat. Prot. Dosim*. **100**, 429–432.

Krása, J., Jungwirth, K., Krouský, E., Láska, L., Rohlena, K., Pfeifer, M., Ullschmied, J. & Velyhan, A. (2007). Temperature and centre-of-mass energy of ions emitted by laser-produced polyethylene plasma. *Plasma Phys. Control Fusion* **49**, 1649–1659.

Láska, L., Krása, J., Mašek, K., Pfeifer, M., Králiková, B., Mocek, T., Skála, J., Straka, P., Trenda, P., Rohlena, K., Woryna, E., Farny, J., Parys, P., Wolowski, J., Mroz, W., Shumshurov, A., Sharkov, B., Collier, J., Langbein, K. & Haseroth, H. (1996). Iodine laser production of highly charged Ta ions. *Czech. J. Phys*. **46**, 1099–1115.

Láska, L., Jungwirth, K., Krása, J., Pfeifer, M., Rohlena, K., Ullschmied, J., Badziak, J., Parys, P., Wolowski, J., Gammino, S., Torrisi, L. & Boody, F.P. (2005). Charge-state and energy enhancement of laser-produced ions due to nonlinear processes in preformed plasma. *Appl. Phys. Lett*. **86**, 081502.

Láska, L., Jungwirth, K., Krása, J., Krouský, E., Pfeifer, M., Rohlena, K., Ullschmied, J., Badziak, J., Parys, P., Wolowski, J., Gammino, S., Torrisi, L. & Boody, F. P. (2006). Self-focusing in processes of laser generation of highly-charged and high-energy heavy ions. *Laser Part. Beams* **24**, 175–179.

Láska, L., Badziak, J., Boody, F. P., Gammino, S., Jungwirth, K., Krása, J., Krouský, E., Parys, P., Pfeifer, M., Rohlena, K., Ryć, L., Skála, J., Torrisi, L., Ullschmied, J. & WoLowski, J. (2007). Factors influencing parameters of laser ion sources. *Laser Part. Beams* **25**, 199–205.

Láska, L., Jungwirth, K., Krása, J., Krouský, E., Pfeifer, M., Rohlena, K., Velyhan, A., Ullschmied, J., Gammino, S., Torrisi, L. K., Badziak, J., Parys, P., Rosinski, M., Ryć, L. & WoLowski, J. (2008*a*). Angular distributions of ions emitted from laser plasma produced at various irradiation angles and laser intensities. *Laser Part. Beams* **26**, 555–565.

Láska, L., Jungwirth, K., Krása, J., Krouský, E., Margarone, D., Pfeifer, M., Rohlena, K., Ryć, L., Skála, J., Torrisi, L., Ullschmied, J. & Velyhan, A. (2008*b*). Laser generation of Au-ions with charge states above 50 + . *Rev. Sci. Instrum*. **79**, 02C 715.

Láska, L., Cavallaro, C., Jungwirth, K., Krása, J., Krouský, E., Margarone, D., Mezzasalma, A., Pfeifer, M., Rohlena, K., Ryć, L., Skála, J., Torrisi, L., Ullschmied, J., Velyhan, A. & Verona-Rinati, G. (2008*c*). Experimental studies of emission of highly charged Au-ions and of X-rays from the laser-produced plasma at high laser intensities. *Eur. Phys. J.D.* doi: 10.1190/epid/e2008-00226-8.

Mackinnon, A.J., Borghesi, M., Hatchett, S., Key, M.H., Patel, P.K., Campbell, H., Schiavi, A., Snavely, R., Wilks, S.C. & Willi, O. (2001). Effect of plasma scale length on multi-MeV proton production by intense laser pulse. *Phys. Rev. Lett*. **86**, 1769–1772.

Maksimchuk, A., Gu, S., Flippo, K., Umstadter, D. & Bychenkov, V.Yu. (2000). Forward ion acceleration in thin films driven by a high-intensity laser. *Phys. Rev. Lett*. **84**, 4108–4811.

Malka, V., Faure, J., Fritzler, S., Manclossi, M., Guemnie-Tafo, A., d'Humieres, E., Lefebvre, E. & Batani (2008). Production of energetic proton beams with lasers. *Rev. Sci. Instrum*. **77**, 03B302.

Margarone, D., Láska, L., Torrisi, L., Gammino, S., Krása, J., Krouský, E., Parys, P., Pfeifer, M., Rohlena, K., Rosinski, M., Ryc, L., Skála, J., Ullschmied, J., Velyhan, A. &

https://doi.org/10.1017/S0263034609000202 Published online by Cambridge University Press

WoLowski, J. (2008). Studies of craters dimension for long-pulse laser ablation of metal targets at various experimental conditions. *Appl. Surf. Sci*, **254**, 2797–2803.

Pukhov, A. & Meyer-ter-Vehn, J. (1996). Relativistic magnetic self-channeling of light in near-critical plasma: Three-dimensional particle-in-cell simulation. *Phys. Rev. Lett.* **76**, 3975–3978.

Ryć, L., Badziak, J., Juha, L., Krása, J., Králiková, B., Láska, L., Parys, P., Pfeifer, M., Rohlena, K., Skála, J., Slysz, W., Ullschmied, J., Wegrzecki, M. & Wolowski, J. (2003). The use of silikon photodiodes for X-ray diagnostics in the PALS plasma experiments. *Plasma Phys. Contr. Fusion* **45**, 1079–1086.

Tallents, G.J., Luther-Davies, B. & Horsburgh, M.A. (1986). EXAFS spectroscopy by continuum soft X-ray emission from a short pulse laser-produced plasma. *Aust. J. Phys.* **39**, 253–270.

Torrisi, L., Gammino, S., Mezzasalma, A.M., Gentile, C., Krása, J., Láska, L., Rohlena, K., Badziak, J., Parys, P., Woryna, E. & Wolowski, J. (2003). Tantalum irradiation by high power pulsed laser at 1315 nm and 438 nm wavelengths. *Appl. Surf. Sci*. **220**, 193–202.

Torrisi, L., Margarone, D., Láska, L., Krása, J., Velyhan, A., Pfeifer, M., Ullschmied, J. & Ryc, L. (2008a). Self-focusing effect in Au-target induced by high power pulsed laser at PALS. *Laser Part. Beams* **26**, 379–387.

Torrisi, L., Margarone, D., Láska, L., Verona-Rinati, G., Milani, E., Cavallaro, C., Ryc, L., Krása, J., Rohlena, K. & Ullschmied, J. (2008b). Monocrystalline diamond detector for ionizing radiation emitted by high temperature laser generated plasma. *J. Appl. Phys*. **103**, 083106.

Ullschmied, J. (2006). Overview of laser plasma experiments at PALS. *Proc. XXIX ECLIM, Madrid*, p.52–60.

Woryna, E., Parys, P., Wolowski, J. & Mróz, W. (1996). Corpuscular diagnostics and processing methods applied in investigations of laser-produced plasma as a source of highly ionized ions. *Laser Part. Beams* **14**, 293–321.

https://doi.org/10.1017/S0263034609000202 Published online by Cambridge University Press